J Appl Physiol 120: 17–28, 2016.
First published October 22, 2015; doi:10.1152/japplphysiol.00543.2015.

Synthesis Review

The role of morphology in mathematical models of placental gas exchange

A. S. Serov,[1] C. Salafia,[2] D. S. Grebenkov,[1] and M. Filoche[1]

[1]*Physique de la Matière Condensée, Centre National de la Recherche Scientifique, Ecole Polytechnique, Palaiseau, France; and* [2]*Placental Analytics, LLC, Larchmont, New York*

Submitted 29 June 2015; accepted in final form 8 October 2015

Serov AS, Salafia C, Grebenkov DS, Filoche M. The role of morphology in mathematical models of placental gas exchange. *J Appl Physiol* 120: 17–28, 2016. First published October 22, 2015; doi:10.1152/japplphysiol.00543.2015.—The performance of the placenta as a gas exchanger has a direct impact on the future health of the newborn. To provide accurate estimates of respiratory gas exchange rates, placenta models need to account for both the physiology of exchange and the organ morphology. While the former has been extensively studied, accounting for the latter is still a challenge. The geometrical complexity of placental structure requires use of carefully crafted approximations. We present here the state of the art of respiratory gas exchange placenta modeling and demonstrate the influence of the morphology description on model predictions. Advantages and shortcomings of various classes of models are discussed, and experimental techniques that may be used for model validation are summarized. Several directions for future development are suggested.

flow patterns; diffusing capacity; porous medium; histomorphometry; experimental techniques

THE PLACENTA IS CRUCIAL FOR fetal development: this multifunctional organ combines respiratory, nutrition, excretion, immune, and endocrine functions. Previous works have convincingly demonstrated that placental morphological and physiological characteristics are related to health of the newborn and the future adult. Both placenta weight and placenta-fetus weight ratio have been associated with newborn health (60, 159), while placenta size has been linked to risks of heart diseases in adults (8). Correlations between placental morphology and intelligence quotient at age 7 yr (109) and risk of hypertension in adults (33) have also been reported. Placental pathologies were shown to be the main cause (64.9%) of intrauterine fetal death after the 20th wk of pregnancy (72). In this situation, analyzing the placenta is of great interest as it may help to determine the origin of fatal outcome, e.g. *1*) an intrinsic placental abnormality (such as maternal floor infarction, umbilical cord knot, or massive chorangioma), *2*) a disease not originated in the placenta but ending in abnormal placental function (such as maternal underperfusion or fetal thrombotic vasulopathy), or *3*) abnormalities of the intrauterine environment (such as hypoxia, diabetes, or preeclampsia) that are reflected in the placenta (for instance, in chorangiosis or increased number of nucleated red blood cells) (7).

While the placenta can be considered as a "witness" (7) or a "diary of gestation life" (5) and may help to assess newborn health risks, this valuable and unique source of information about fetal development is usually discarded after birth as medical waste. At the same time, it is the only organ that is not needed after birth and, thus, can be extensively analyzed postpartum.

Mathematical models of exchange across the placenta have been proposed for more than six decades. Most models focused on respiratory gas exchange, since compromised exchange of respiratory gases has the most immediate fetal impact (within a minute) and as a worst case may lead to permanent brain damage or fetal death (16, 47, 128, 132). It was also argued that alterations of placental morphology due to pathological conditions (such as diabetes and preeclampsia) are correlated with placental gas exchange efficiency (31, 63, 79, 97, 101, 103). The primary goal of respiratory gas placenta models is to provide a quantitative description of the placental exchange and to estimate its efficiency based on the available experimental data. Once these estimations achieve a certain level of precision, they could be used in medical diagnosis of pathologies of fetal development and assessment of newborn health risks. Finally, some predictions of respiratory gas exchange models (especially those related to organ morphology) can be extended to the exchange of other substances once substance-specific transport mechanisms are taken into account.

Models normally include two main aspects: physiology of respiratory gas transport and placental morphology as an exchanger. The physiological part includes gas diffusion in blood plasma in placental tissues and across placental membranes, as well as kinetics of placental tissue respiratory metabolism and Hill's law of hemoglobin dissociation, all of which are well studied. In contrast, accounting for organ geometry in respiratory gas exchange models is still challenging.

The internal structure of the placenta is complicated. Each placenta consists of a maternal and a fetal part, but their organization varies with species. In many species, maternal blood and fetal blood pass through the placenta in blood vessels that come into close contact to allow exchange. Such organization is found in epitheliochorial (horse, pig), synepitheliochorial (ruminants), and endotheliochorial (dog, cat) pla-

Address for reprint requests and other correspondence: M. Filoche, Laboratoire de Physique de la Matière Condensée, Ecole Polytechnique, CNRS, 91128 Palaiseau Cedex, France (e-mail: marcel.filoche@polytechnique.edu).

centas, where two or more tissue layers separate maternal from fetal placental vascular systems (69). However, the structure of a hemochorial labyrinthine placenta (human and primate) is quite different, since maternal blood is not confined to vessels and directly bathes fetal tissues. Such structural organization significantly complicates description of transport properties of these placentas. This review mainly focuses on the human placenta because of its primary medical interest and because of the greater complexity of the human placenta structure compared to other species (for a review of placental anatomy of other species the reader is referred to Refs. 14, 69). It should be noted that some results obtained for animal placentas are still applicable to human placentas on a very small scale (several villi).

Let us examine in more detail the interplay between gas exchange and morphometry of the human placenta. A healthy human placenta at term is a disk with an average diameter of 22 cm (15). The two faces of the disk are called the chorionic plate (from which the umbilical cord stems) and the basal plate (that anchors the placenta to the uterus) (see Fig. 1). The average thickness of the placenta postpartum is 2.5 cm (the placenta in vivo is up to 2 times thicker), and the average weight is 470 g. In regards to internal structure, the maternal portion of the placenta is a basin into which maternal blood is brought by 50-120 spiral arteries with 100–500 orifices (117) and which is drained by around 30 decidual veins with around 80 openings (Fig. 1; see Refs. 15, 42). The fetal portion is a tree of villi with up to 30 generations of branches (mean value of ~10; see Ref. 15) immersed in maternal blood. According to caliber, stromal structure, vessel structure, and location within the villous tree, four major villi types are distinguished: stem villi (300-3,000 μm in diameter), immature intermediate villi (60–200 μm), mature intermediate villi (40–80 μm), and terminal villi (30–80 μm). Inside each villus, fetal vessels conduct fetal blood from the umbilical arteries to the umbilical vein without admixture with maternal blood. All exchange processes take place at the surface of the fetal villi, mainly in the smallest branches of the tree (terminal and mature intermediate villi) in which fetal capillaries are located close to a thin villous membrane (15). A small typical cross section of the fetal villous tree of a healthy human placenta is shown in Fig. 2*B*. Under pathological conditions, the "healthy" proportions of various placental components in Fig. 2*B* may be altered and feature, for instance, disproportionally large intervillous space and rare villi in preeclampsia (Fig. 2*A*) or denser and larger villi in diabetes (Fig. 2*C*).

The human placenta at term is normally described as subdivided into 40–60 functional units (placentones, also called lobules or cotyledons) with a characteristic diameter of 3.5 cm, which are not completely separated from each other (15). Each placentone typically has a villi-free central cavity of ~1.5 cm in diameter into which spiral arteries open, while the draining decidual veins tend to be located at the periphery of the placentone (at the basal plate or in the placental septa; see Fig. 1 and Ref. 15). The central cavity is believed to be formed by a "jet" of arterial maternal blood spurting from the spiral arteries at a linear velocity of ~10 cm/s (see discussion in Refs. 15, 18, 23, 127).

The above description concerns the human placenta at term, but the placenta continuously grows with the fetus, and its structure and function evolve in time. The maternal circulation starts in the human placenta only around 10th-12th week of gestation, after maternal spiral arteries have been invaded and remodeled by fetal trophoblasts (see Refs. 15, 23). This delayed onset of maternal circulation is believed to protect the developing fetal tissues from the high velocity of maternal blood flow and high partial pressures of oxygen. Most mathematical models focus on gas exchange in the term human placenta, since extensive data about this stage can be obtained by analyzing the freshly delivered organ.

To be used in numerical computations, the complicated placental structure needs to be simplified. The challenge con-

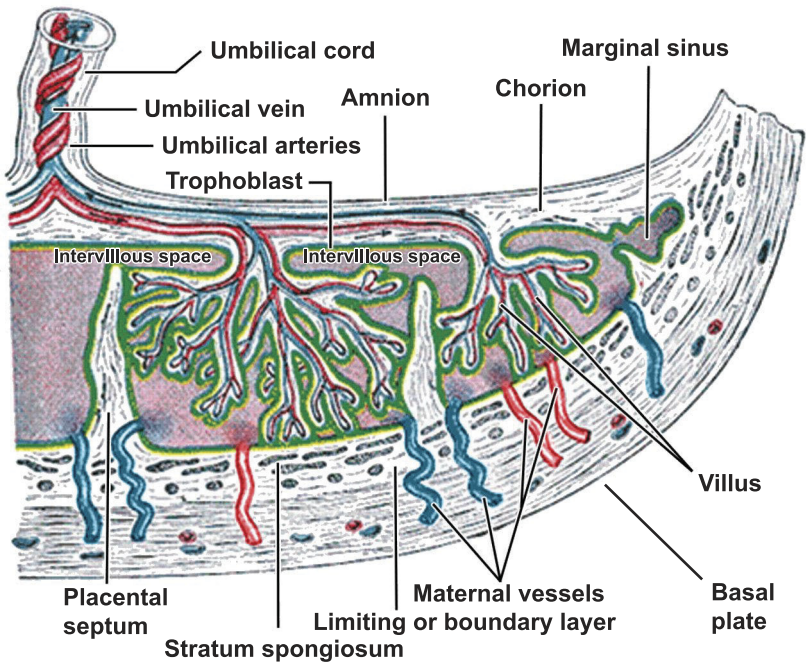

Fig. 1. Structure of the human placenta (modified from Ref. 49). The lower side is the basal plate that attaches to the uterus; the upper side is the chorionic plate, where the umbilical cord connects to the placenta.

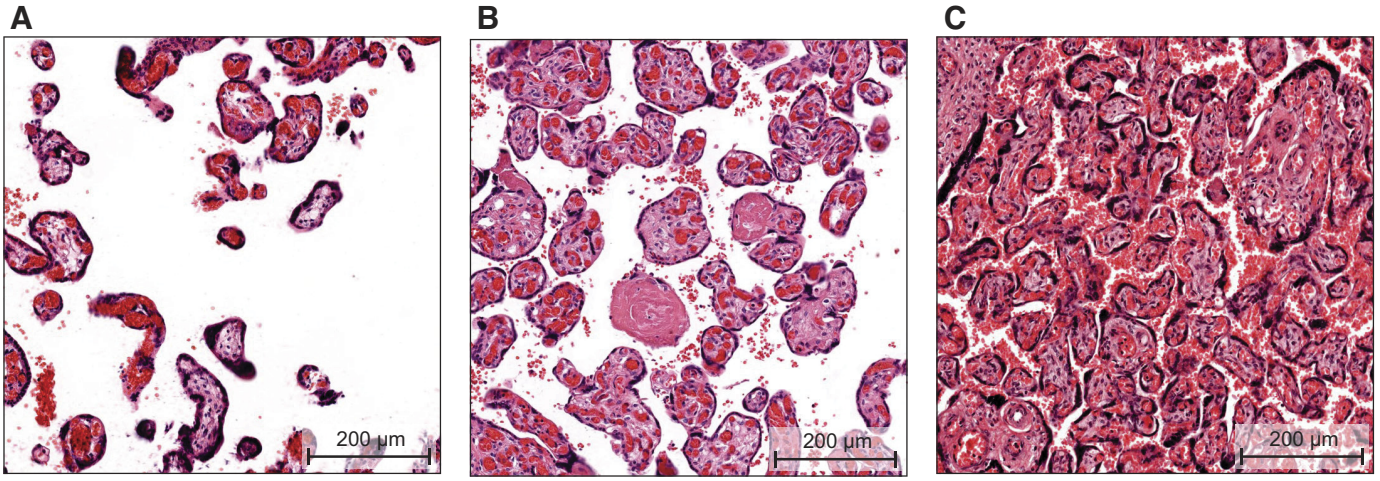

Fig. 2. Small fragments of typical 2D histological cross sections of the human placenta: preeclamptic placenta (sparse villi, reduced exchange surface; *A*), healthy placenta (*B*), and diabetic placenta (densely packed villi, reduced surface accessibility; *C*). Note, however, that due to a very heterogeneous structure, a healthy placenta may also contain regions similar to those shown in plates *A* and *C*, but their fraction is typically much lower. In all three images, the white space corresponds to the intervillous space, normally filled with maternal blood, which has been washed away during the preparation of the slides (some residual red blood cells are still present). The large red shapes are the cross sections of the fetal villi. Redder regions inside correspond to fetal capillaries. Histological cross sections are normally taken in the direction from the basal plate to the chorionic plate (see Fig. 1) and are stained with hematoxylin and eosin.

sists in finding a proper balance between oversimplification (too far from the physiological reality) and an overdetailed model (computationally unworkable). With time, gas exchange placenta models have evolved through the following stages, each corresponding to an increased complexity of the morphology description: *1*) *capillary-scale (compartmental) models* and *studies of flow patterns*, *2*) *morphometric diffusing capacity models*, *3*) *distributed-parameters models* (including *porous-medium models*), and *4*) *models based on histological placental cross sections*.

In the following sections, we discuss these stages of evolution, focusing on advantages of each approach and emphasizing drawbacks that required further progress. A separate section of the review is devoted to experimental techniques and data available for validation of the models. In the last section, we discuss geometrical features of the placenta that should be accounted for in future models.

Models of Placental Respiratory Gas Exchange

Capillary-scale models; flow patterns. Capillary-scale placenta models were the first models of respiratory gas exchange. They capitalized on anatomical observations that placentas of different species feature different co-orientations of maternal and fetal blood flows, and explored how this fact may influence exchange properties of the organ. These compartmental models distinguished five principal flow patterns (see Fig. 3 and Ref. 34): *1*) pool flow (a uniform solute concentration along the length of maternal or fetal capillaries), *2*) double pool flow (uniform solute concentrations in both maternal and fetal capillaries), *3*) countercurrent flow, *4*) concurrent flow, and *5*) cross-current flow (or multivillous flow: maternal capillaries perpendicular to fetal capillaries). Anatomical studies suggest that the guinea pig and rabbit placentas are well represented by the countercurrent pattern, the goat and sheep placentas are venous equilibrators sharing features of the concurrent and pool flow patterns (35, 36, 168), and the human and primate placentas can be approximated by the multivillous flow pattern (although maternal blood is not confined to capillaries in these placentas). The exchange efficiency of the different flow patterns was compared, and it was demonstrated that the countercurrent flow pattern provides the highest exchange rate (12–14, 52, 55, 75, 107, 115, 145, 152, 168, 169). This conclusion, inter alia suggesting higher exchange rate in the guinea pig placenta than in the human placenta, questions definitions of efficiency and robustness of placental gas exchange and how they can be compared across species (see discussion in Refs. 36, 39).

The development of flow pattern studies continued with introduction of dimensionless exchange parameters (*transport fraction*, *flow ratio*, *placental permeability*, and *placental clearance*) used to compare experimental data on solute exchange in different species (12, 14, 34–36, 38, 104, 108, 123, 129, 130, 145) and to discuss the two specific cases of *diffusion-limited* (or *permeability-limited*) and *flow-limited* placen-

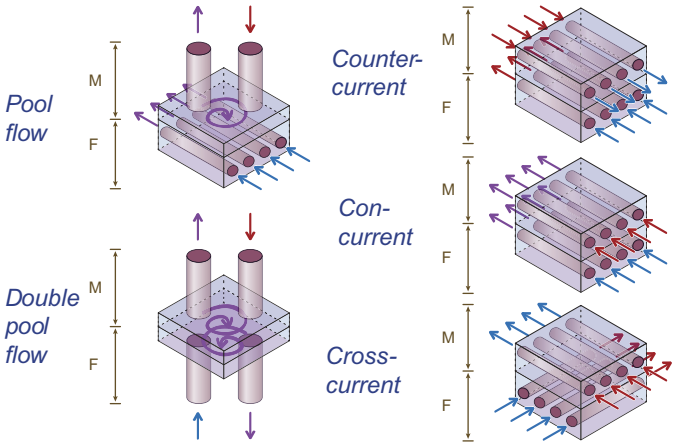

Fig. 3. Five principal patterns of blood flow based on the original scheme by Faber (34). The letters F and M mark fetal and maternal parts of the exchangers respectively. Arrows show the direction of the blood flows. Their color indicates high (red), intermediate (violet), and low (blue) blood oxygenation (for more details see Ref. 34 and references therein).

tal exchange (14, 104). More details on flow patterns can be found in Ref. 14, where experimental data are also summarized.

Flow-pattern models have been further used to study influences of different physiological and geometrical parameters on placental respiratory gas and other substance exchange (11, 13, 24, 28, 34–37, 50–53, 55, 57, 58, 70, 75, 78, 85, 86, 88–90, 107, 108, 110, 121–124, 129, 130, 134, 143, 145, 147, 152, 156, 167). However, they oversimplify placental geometry, focusing on dynamics of gas concentration in fetal and maternal blood considered as two compartments separated by a single effective membrane. This approach could not account for the complexity of the diffusion path of respiratory gases, and new, *morphometric diffusing capacity models*, had to be introduced.

Morphometric diffusing capacity models. In these models the oxygen diffusion path in human placentas was considered as consisting of five geometrical compartments in series (Fig. 4): *1*) maternal red blood cells (me), *2*) maternal blood plasma (mp), *3*) villous membrane, comprising the syncytiotrophoblast layer, the basement membrane, the villous stroma and the fetal capillary endothelium (vm), *4*) fetal blood plasma (fp), and *5*) fetal red blood cells (fe). The mathematical language of the models had to be adapted to this multistage description.

For a single membrane, *membrane permeability* is defined as the proportionality constant between the rate of transfer per unit of membrane surface and the solute concentration difference on both sides of the membrane. Permeability is hence a local characteristic defined per unit of surface. However, for a multistage (and multimembrane) process, it is necessary to also introduce a quantity characterizing exchange in the placenta as a whole, such as a *placental permeability*, defined as the total flow rate across the placenta per unit of mean concentration difference between fetal and maternal circulations (36). For respiratory gases, this rate is traditionally measured in milliliters per minute, and the concentration difference is replaced by the partial pressure difference in millimeters of mercury, with the resulting quantity called the *placental diffusing capacity* D_p (with index p referring to the placenta).

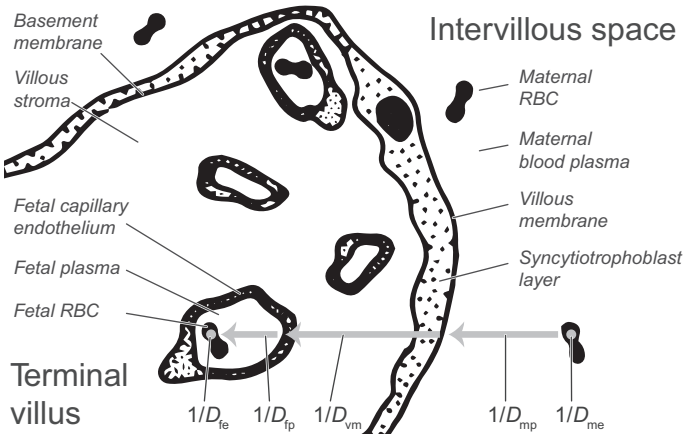

Fig. 4. A schematic cross section of one fetal terminal villus illustrating the components of the complex respiratory gas diffusion path. Notations are explained in the text. The internal part of fetal villus and red blood cell distributions are simplified. Based on the original scheme by Mayhew et al. (98).

First calculations in the human placenta yielded $D_p \approx 0.5$ ml/(min·mmHg) (12, 13). However, these estimations oversimplified the diffusion path and did not rely on precise morphometric data, and were later refined by Hill et al. (57), Laga et al. (73), and Longo et al. (87, 88). These authors calculated diffusing capacity with a serial resistance model (see Fig. 4):

$$\frac{1}{D_p} = \frac{1}{D_{me}} + \frac{1}{D_{mp}} + \frac{1}{D_{vm}} + \frac{1}{D_{fp}} + \frac{1}{D_{fe}}, \qquad (1)$$

where the reciprocal of total diffusing capacity for oxygen is assumed to be the sum of reciprocals of the diffusive capacities of each of the path components. For each of the components, Laga et al. (73) provided an approximate expression in terms of geometrical characteristics of villi and the intervillous space (IVS). Efficiency of oxygen exchange was thus related to placental morphology through the dependence of diffusive resistance on geometrical parameters. In particular, it was shown that placental diffusional exchange performance is essentially determined by three measurable structural quantities: mean harmonic thickness of the villous membrane (defined as the reciprocal of the arithmetic mean of membrane thickness reciprocals), villous surface area, and fetal capillary surface area.

Typical values of the diffusing capacity D_p were found to lie in the 3–5 ml/(min·mmHg) range: 3.1 ml/(min·mmHg) in Ref. 73, 5.1 ml/(min·mmHg) in Ref. 98, and 3 ml/(min·mmHg) in Ref. 99. It was also demonstrated that the villous membrane accounts for ~90% of diffusive resistance $1/D_p$, which confirmed earlier findings (12, 13). Note that the obtained values of D_p depend on the used fixation and histomorphometrical techniques. These results were matched to physiological measurements and compared with calculations by other groups (1, 73, 74, 100, 101, 157, 158). It should be mentioned here that independent physiological experiments indicate that oxygen exchange in the human placenta and placentas of other species is flow limited rather than diffusion limited (36, 39). This observation suggests that the obtained value of D_p is large enough to allow practically all oxygen brought by the maternal circulation to be transferred across the placental barrier. However, this point of view is not shared by all investigators (168).

The definition (1) of morphometric placental diffusing capacity (D_p) is similar to the formula that describes the morphometric diffusing capacity of the lung (D_L) earlier introduced by Roughton and Forster (138) and Weibel (162, 163). Since both the lung and the placenta supply the same living organism with oxygen at different stages of its development, it might be instructive to compare their diffusing capacities. The diffusing capacity D_{LO_2} of an adult human lung at rest is reported to be ~30 ml/(min·mmHg), reaching as much as 100 ml/(min·mmHg) at heavy exercise (164, 165). Recalculated per kilogram of body tissue, D_{LO_2} values give a diffusing capacity ~0.45 ml/(min·mmHg·kg) at rest and 1.4 ml/(min·mmHg·kg) under exercise for a 70-kg adult. For the placenta, recalculation of $D_p \approx 3$–5 ml/(min·mmHg) per kilogram of fetal weight at term (3.2 kg on average, see Ref. 140), gives 0.95–1.55 ml/(min·mmHg·kg). This value is similar to that of the adult human lung under exercise conditions. Note finally that oxygen transport in the lung under normal conditions is also flow limited (166).

Morphometric diffusing capacity models present a significant improvement over capillary-scale models, since they are able to provide case-specific estimates of overall human placental oxygen exchange rate based on histological placental data. However, the 1D geometry of these models does not allow proper consideration of convective transport of oxygen, which may create significant variations of oxygen concentration in different parts of the IVS. To explore maternal blood flow distribution in the human placenta and its impact on oxygen uptake, *distributed-parameters models* were proposed.

Distributed-parameters models. One of the first models of this class was introduced by Aifantis (2), who treated mass transport in the human placenta as a mixture problem. The placental tissue was considered as a solid constituent, while fetal blood and maternal blood were modeled as two fluid constituents. These three components were allowed to interact in a general way chemically, mechanically, and thermally according to the laws of mass, momentum, and energy conservation. This model is, however, only a general framework; case-specific calculations are required to relate the model to the experiment.

One possible way of introducing properties of solid and fluid constituents is to consider the intervillous space as a porous medium with maternal blood percolating through it. Mathematically, such description can take the form of Darcy's law, which assumes a linear relation between flow velocity, hydrostatic blood pressure, and porosity of the solid component (119). A theoretical discussion of the applicability of porous-medium models to the human placenta from a hydrodynamic point of view and a method of calculating porous-medium parameters from histological placental cross sections can be found in Refs. 25–27, 143.

The first calculation of distribution of the maternal blood flow in a porous-medium human placenta model was performed by Erian et al. (32). This model describes a square porous-medium placentone through which maternal blood percolates following Darcy's law (Fig. 5*A*). Several permeability configurations were solved, which all yielded significantly nonuniform (and hence inefficient) perfusion of the placentone by maternal blood. In particular, it was observed that a portion of maternal blood directly flowed from the spiral artery to decidual veins without penetrating deep into the placentone. This *short-circuiting* was attributed to the fact that inertia of flow was disregarded (Darcy's law) and that pulsatility of maternal blood flow was ignored. However, other explanations are also possible: *1*) the chosen ad hoc form of the velocity dependence of the permeability may not rightly represent villi

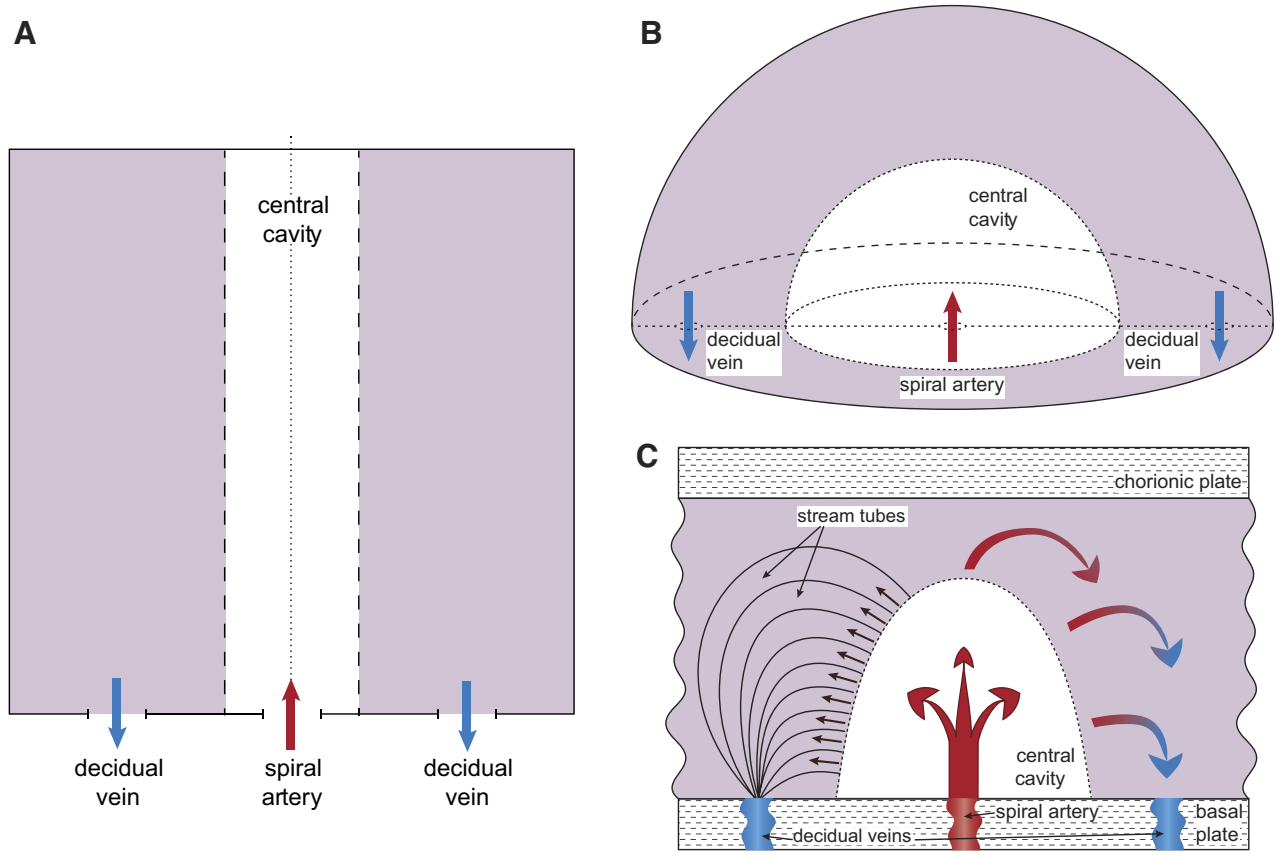

Fig. 5. *A*: scheme of a square 2D placentone filled with a porous medium as proposed by Erian et al. (32). One spiral artery and 2 decidual veins were placed at the bottom of the placentone. The boundary of the central cavity is marked by 2 dashed lines. An extension to a cylindrical 2D + 1D model by rotation around the central "vertical" axis (dotted line) was proposed. *B*: scheme of the hemispherical 3D porous-medium placentone model of Chernyavsky et al. (26). A dotted line delimits the central cavity. The same number and location of maternal vessels as in *A* was used. Rotational symmetry was assumed around the "horizontal" axis passing through the three vessels. *C*: scheme of stream tubes location in the placentone model of Serov et al. (150). Each stream tube (at *left*) corresponds to a small part of the whole maternal blood flow. At *right*, a gradual transformation of the maternal blood from arterial into venous is schematically demonstrated.

properties or *2*) the description of the placenta as a porous medium may be inadequate.

To understand which of these explanations is correct and why the model of Erian et al. (32) predicted inefficient placentone perfusion, a modified 3D placentone model was constructed, and the influence of location and size of the maternal veins on the blood flow distribution in the placentone was studied (Fig. 5*B*; see Ref. 26). The porous medium was considered nondeformable, which allowed for an analytical calculation of maternal blood flow distribution. To model placental exchange, a uniform volumetric absorption coefficient was assumed everywhere outside the central cavity. However, no account for specific transport kinetics of the solute (e.g., oxygen-hemoglobin dissociation) was given, so that model application was limited to transport of inert solutes (the authors' choice of oxygen dissolved in the blood plasma as an illustration of inert solute transport being confusing).

Three main conclusions were drawn: *1*) If decidual veins are located near the periphery of the placentone, maternal blood flow penetrates deeper into the IVS and rather efficiently perfuses the placentone. In other words, even with no account for flow inertia, more efficient perfusion of the placentone can be obtained by the correct positioning of venous outlets with respect to the arteries. *2*) There is an optimal size of the central cavity that is a compromise between hydraulic resistance to maternal flow and the amount of villous tissue participating in solute uptake. *3*) There is also an optimal volume fraction of "villous material" in the IVS as a result of trade-off between flow resistance and the uptake capacity of a placentone. However, the obtained value of optimal villi density corresponds to high-altitude or preeclamptic placentas rather than to healthy ones (26, 150).

In summary, the porous-medium approach was proved valuable for estimating maternal blood flow distribution in the placentone and analysis of the effects of shear stress and flow resistance. However, the porous medium concept imposes several serious limitations. *1*) It is difficult to model respiratory gas uptake due to the absence of a clearly defined uptake surface. *2*) Darcy's law that neglects diffusive transport of solutes in the IVS may be not valid for low maternal blood velocities in small IVS pores. *3*) Human placenta morphology is represented as random, which ignores the branching tree-like structure of the villi. Addressing these issues required conception of a new type of model, *models based on histological placental cross sections*.

Models based on histological placental cross sections. Geometrical models reviewed below are based on 2D histological placental cross sections (Fig. 2) and hence feature a clearly defined uptake surface. A model of intravillous oxygen transport was first proposed by Gill et al. (46), who used 2D spatial distributions of capillaries in several dozens of villi manually traced in histological cross sections of the human placenta. Uniform oxygen concentration was assumed on the perimeter of all villi, while perfect sink conditions were set on capillary boundaries. Purely diffusive oxygen transport was then simulated. Calculations showed that fetal capillaries located close to the center of a villus have smaller contribution to uptake of the villus than those located near the villous boundary, and this effect was named *screening of capillaries* analogous to the screening concept in the lungs (40, 142). A *villus efficiency* was then introduced, which may be potentially correlated to independent indicators of the placental exchange efficiency, such as the placenta-fetus birth weight ratio.

However, exchange efficiency calculated in this way may be strongly affected by variations of oxygen concentration at villous boundaries in different regions of the IVS, which are not accounted for in this model. To study oxygen transport in the IVS, diffusion and convection have to be considered simultaneously, and for this purpose it was found convenient to subdivide the whole pattern of the maternal blood flow into small stream tubes (see Refs. 149–151 and Fig. 5*C*). Each stream tube describes a path that a small volume of blood follows while moving from a spiral artery to a decidual vein and that is crossed by villi of arbitrary cross sections. Calculations made with this model demonstrated that trade-off between the amount of oxygen coming into the stream tube and the absorbing villous surface inside it yields an optimal villi density maximizing oxygen uptake. This optimal villi density has a different origin from that proposed in the porous-medium approach and was shown to correspond to villi density observed on average in a healthy human placenta (150).

While giving realistic predictions of villi density, the stream-tube placenta model has the following limitations: *1*) its results were obtained with slip boundary conditions (nonzero velocity at the blood-tissue interface); *2*) internal villous structure was disregarded (fetal blood circulation was ignored and perfect-sink conditions were assumed at the villi boundaries), and *3*) geometry of stream-tube cross sections was assumed to be invariant along the maternal blood flow. Further studies are necessary to assess the influence of these assumptions on the obtained results.

Comparison with Experiment

After this overview of the evolution of morphologic description in respiratory gas exchange placenta models, one may wonder how well predictions of these models correspond to medical observations and experimental measurements. One should take into account that a limited number of measurements are ethical in the human placenta in vivo, with most measurements being available only after birth. In what follows, we summarize experimental techniques and results that are currently available either on a regular basis, or in clinical research, and review the ways of experimental validation of the models. Note that there exist many discrepancies within results of experimental studies, which are mainly due to inconsistent techniques of investigation (such as different ways of placental fixation, calculation of placental parameters, or umbilical cord clamping) or biological variations.

1) Macroscopic measurements such as placental weight, placenta-to-fetus weight ratio, placental diameter and thickness can be obtained after birth (see, for example, Ref. 109).

2) Histomorphometric measurements can be manually performed on histological placental cross sections obtained after birth (see Refs. 73, 146 and references therein). These studies report differences in placental morphometry between healthy and pathological placentas (similar to those shown in Fig. 2). Note, however, that placental morphometry obtained after birth may not exactly represent the in vivo situation, because of detachment of the placenta from the uterine wall, cessation of maternal blood flow, mechanical stress of vaginal delivery, and fixation procedures (21, 22, 61, 67, 91, 96, 102).

3) Placental corrosion casts can be prepared (80–82) providing several generations of fetal villous tree branches. They can then be analyzed, in particular, by means of scanning electron microscopy (20, 54, 68). Such corrosion casts can be used for visualizing fetal vasculature, but do not provide information about villi surfaces or small villous tree branches.

4) Confocal laser scanning microscopy with 3D reconstruction can be used to qualitatively and quantitatively compare terminal villi structure in healthy and pathological placentas (see Refs. 64, 137 and references therein).

5) Artificial placenta perfusion can be performed after birth to imitate in vivo placental function (65, 144). However, this method requires that placental membranes are not damaged (which is often an issue with vaginal deliveries) and does not support long perfusion times.

6) Partial pressures of oxygen, carbon dioxide, and concentrations of other solutes, as well as volumetric blood flows in uterine and umbilical arteries and veins can be measured in multiple species (see Refs. 35, 36 and references therein).

7) X-ray photographs of in vivo placenta perfusion by the maternal blood have been obtained with a radioactive dye in normal and pathological human pregnancies and in primates (19, 43–45, 126, 127). The resulting data provide evidence for the existence of a central cavity and allow estimation of characteristic size of a placentone, transit time of blood through the IVS, and an average velocity of maternal blood flow (150). However, X-ray involving techniques are now unethical and are used in humans only in serious pathological conditions.

8) Standard ultrasound techniques provide placental size, shape, and volume in utero. Typical values of linear blood velocity and pulsatility indexes in umbilical and uterine arteries and veins, as well as in spiral arteries, can also be obtained (see Ref. 62 and note that mathematical models often require linear blood velocities rather than the integral blood flow). However, the sensitivity threshold of these techniques to linear flow velocities is ~0.1 cm/s, which is insufficient to measure the blood velocities expected in the IVS (~0.05 cm/s on the average, see Ref. 150). The use of potentially safe contrast agents (e.g., microbubbles of inert gas) may enhance their resolution (125).

9) Ultrafast ultrasound techniques are likely to allow high-sensitivity mapping of blood flows simultaneously in the whole placenta analogous to brain studies (29), with the possibility of distinction between fetal and maternal blood by analyzing pulsatility indices.

10) 3D color/power Doppler angiography is able to provide a low-resolution villous tree structure and patterns of blood flow in the vicinity of central cavities (71). It can also be used for reproducible quantification of placental and myometrial vascularization (113, 114). Color Doppler sonograms measure linear blood velocity and its direction (to or from the sensor), while power Doppler signals are proportional to the sum of velocities of all scatterers in a region (with a resolution of up to 0.1 cm/s) and are independent of the angle of insonation (30). Based on the power Doppler method, 2D and 3D *fractional moving blood volume* techniques were proposed to assess the fraction of moving blood in the placenta (139, 155).

11) T1- and T2-weighted contrast MRI techniques can be used to determine placental location in vivo and the main blood circulation regions (84, 94, 116, 170). Higher precision is achieved in animal models by using contrast agents, which allow for visualization of placental perfusion (141). Alternatively, diffusion of water molecules in the placenta can be observed with diffusion-weighted MRI (17, 93). The resulting data can be further analyzed by means of intravoxel incoherent motion (IVIM) models that provide estimates of placental blood volume (4, 111, 112). Similarly, the arterial spin labeling (ASL) method is used to study placental microflow patterns (6), while oxygen-enhanced MRI and blood-oxygen-level-dependent MRI (BOLD MRI) techniques allow one to estimate placental blood oxygenation in vivo (59, 153, 154). Additionally, high-resolution ex vivo MRI angiography is able to provide 3D structure of the human placenta up to the sixth generation of villous branching (131). Analysis of the sensitivity of MRI techniques shows that spatial resolution of MRI methods of ~1 mm is enough to locate main fetal placental vascular structures but would not resolve villi structure in dense exchange regions (with a characteristic villous component size of ~50 μm).

12) Microcomputed tomography techniques can be used to obtain 3D spatial organization of placental arteries and veins, as demonstrated on placentas of small rodents (135, 136) and in humans (76, 77).

Based on available experimental techniques, the following strategies for validating respiratory gas exchange models have been proposed (in addition to those mentioned in previous sections). Battaglia and Meschia (14) suggested measuring maternal and fetal placental blood flows and transplacental diffusion rates of various test molecules and their concentrations in arteries and veins of both mother and fetus to integrally characterize the exchange in placentas of various species. This experimental program was later realized in the sheep model (104, 105). Longo et al. (88, 90) compared predictions of their oxygen and carbon dioxide exchange model to results of in situ perfusion of an isolated placentone (89, 120). Chernyavsky et al. (26) demonstrated that radioactive dye diffusion patterns of Freese (43) observed in the human placenta can be explained by a porous-medium placenta model. Comparison with histological cross sections showed that optimal density of "villous material" of ~30% calculated by Chernyavsky et al. (26) corresponds to pathological rather than healthy placentas, while the villi density of ~47% obtained by Serov et al. (150) correlates well with histological measurements.

Perspectives

Starting with a pair of "capillaries" conducting all fetal and maternal blood, placenta models have evolved to describing the organ as a porous medium or a set of stream tubes whose geometry is based on histological placental cross sections. Mathematical modeling has allowed to predict blood flow distribution and respiratory gas exchange rates in the placenta across different species.

However, our knowledge of gas exchange processes in the complex placental morphology still remains very incomplete. Further development in the field may move in two principal directions. On one hand, porous-medium models should *1*) account for inhomogeneity of villi density observed in histological placental cross sections, *2*) analyze shear stress exerted on villi by blood flow, *3*) account for deformability of villous tissue by introducing a velocity-dependent permeability, *4*)

study the influence on oxygen uptake of the lateral venous outlets in placental septa at placentone borders, or *5*) go beyond a single placentone to describe blood flow patterns in the whole placenta.

On the other hand, nonporous-medium models should *1*) improve representation of placental geometrical structure (e.g., by introducing branching of villi and variations in their shapes, sizes and orientations), *2*) simultaneously account for maternal and fetal circulations by combining developed maternal transport models with fetal transport models, *3*) develop placental structure acquisition and analysis techniques capable of providing case-specific input for models, *4*) evaluate influence on oxygen uptake of slip and nonslip boundary conditions (with respectively nonzero and zero blood velocity) imposed on the villous tree surface, *5*) investigate villi screening in the IVS, and *6*) explore influence of variations of maternal blow velocity in the IVS.

Both porous-medium and nonporous-medium approaches could provide more accurate predictions by incorporating models of structure of villous tree, fetal placental circulation, and umbilical cord circulation (3, 41, 48, 66, 133, 156, 161), of maternal blood flow in the spiral arteries (23, 148), or of the signaling pathways and placental biochemistry (92, 160). It is also important to construct placental models of gas exchange not only at term, but earlier in the course of pregnancy, since developmental pathologies at these stages may cause those seen at later stages. Recent advances in in vivo placental imaging techniques may provide ground for formulation of new early pregnancy gas exchange models.

A promising direction of development of all model types consists in analysis of efficiency and robustness of placental gas exchange. Although the definitions of these notions are debatable and depend on the model, calculation of efficiency and robustness is required for a quantitative comparison of respiratory gas transport in different patients and for identification of cases of pathological placental function. This research axis may lead to important discoveries similar to those made in the human lung (95, 142). Some efficiency criteria, such as the *coefficient of oxygen utilization* (9, 10, 56, 106), the *integrated mean diffusion pressure gradient* (75), the *maternal and fetal transport fractions* (34–36), the *capillary screening coefficient* (46), the *villi density* (26, 150), or *efficiency diagrams* (149, 151) have already been proposed and may serve as a base for future theoretical and experimental studies.

The development of mathematical placenta models is also hindered by missing or insufficient experimental data crucial for validation of the models: *1*) the high-resolution 3D geometrical structure of the placenta is yet unavailable for large placental regions (with at least a thousand villi), especially in dense exchange regions. Meanwhile, models can be based on high-resolution 2D histological cross sections, on low-resolution 3D structures obtained by ex vivo MRI angiography or micro-CT, or on the local high-resolution 3D villi geometry (about dozens of villi) provided by the confocal laser microscopy. *2*) High resolution blood flow patterns in the human placenta have not yet been experimentally determined either in vivo or in vitro. *3*) Oxygen, carbon dioxide, and other substances levels are not available on a regular basis either in the intervillous space of the human placenta or in umbilical and uterine arteries and veins. *4*) There currently exists no automatic image-processing technique for analysis of histological placental cross sections that can provide large histomorphometrical statistics and feed models based on histological cross sections and porous medium models with input data. *5*) The degree to which formaldehyde-fixed histological cross sections faithfully represent in vivo placental structure and the methodologies to correct for possible discrepancies are yet to be established. Advances in these directions would facilitate validation of existing models and stimulate development of new and more accurate ones.

It should be finally noted that respiratory gas exchange models (focusing on geometrical structure of the placenta) can also be applied to studies of transport of other substances if combined with models of substance-specific transport mechanisms, such as amino acids (83, 118, 147), glucose (11), or water (37, 167).

Conclusion

More than six decades of placenta modeling have significantly contributed to a better understanding of the organ function. Modern mathematical models aim not only to describe placental exchange based on available experimental data but to propose quantitative criteria of placental exchange efficiency that would allow diagnosing pregnancy pathologies. In the future, they may become a novel, powerful, and efficient tool in routine analysis of human placentas helping to identify placental pathologies and to assess pregnancy and newborn health risks.

GRANTS

This study was funded by the International Relations Department of Ecole Polytechnique, by Placental Analytics, SAMOVAR Project of the Agence Nationale de Recherche No. 2010-BLAN-1119-05, and Agence Nationale de Recherche Project No. ANR-13JSV5-0006-01. The funding sources have not directly influenced the research process.

DISCLOSURES

C. Salafia is founder and head of Placental Analytics, LLC. There is no conflict of interest involved in Dr. Salafia's contribution to this manuscript.

AUTHOR CONTRIBUTIONS

Author contributions: A.S.S., C.S., D.S.G., and M.F. conception and design of research; A.S.S., C.S., D.S.G., and M.F. analyzed data; A.S.S., C.S., D.S.G., and M.F. interpreted results of experiments; A.S.S., C.S., D.S.G., and M.F. prepared figures; A.S.S., C.S., D.S.G., and M.F. drafted manuscript; A.S.S., C.S., D.S.G., and M.F. edited and revised manuscript; A.S.S., C.S., D.S.G., and M.F. approved final version of manuscript.

REFERENCES

1. **Aherne W, Dunnill MS.** Quantitative aspects of placental structure. *J Pathol Bacteriol* 91: 123–139, 1966.
2. **Aifantis EC.** Towards a rational modeling for the human placenta. *Math Biosci* 40: 281–301, 1978.
3. **Alastruey J, Sherwin SJ, Parker KH, Rubens DD.** Placental transfusion insult in the predisposition for SIDS: a mathematical study. *Early Hum Dev* 85: 455–459, 2009.
4. **Alison M, Chalouhi GE, Autret G, Balvay D, Thiam R, Salomon LJ, Cuenod CA, Clement O, Siauve N.** Use of intravoxel incoherent motion MR imaging to assess placental perfusion in a murine model of placental insufficiency. *Invest Radiol* 48: 17–23, 2013.
5. **Altschuler G.** Some placental considerations in alleged obstetrical and neonatology malpractice. In: *Legal Medicine*, edited by Wecht CH. Salem, MA: Butterworth Legal, 1994, p. 27–47.
6. **Avni R, Raz T, Biton IE, Kalchenko V, Garbow JR, Neeman M.** Unique in utero identification of fetuses in multifetal mouse pregnancies

by placental bidirectional arterial spin labeling MRI. *Magn Reson Med* 68: 560–70, 2012.
7. **Baergen RN.** The placenta as witness. *Clin Perinatol* 34: 393–407, 2007.
8. **Barker DJ.** Fetal origins of coronary heart disease. *Br Med J* 311: 171–174, 1995.
9. **Barron DH.** Some aspects of the transfer of oxygen across the syndesmochorial placenta of the sheep. *Yale J Biol Med* 24: 169–190, 1951
10. **Barron DH, Meschia G.** A comparative study of the exchange of the respiratory gases across the placenta. *Cold Spring Harb Symp Quant Biol* 19: 93–101, 1954.
11. **Barta E, Drugan A.** Glucose transport from mother to fetus a theoretical study. *J Theor Biol* 263: 295–302, 2010.
12. **Bartels H, Moll W.** Passage of inert substances and oxygen in the human placenta. *Pflüg Arch Gesamte Physiol Mensch Tiere* 280: 165–177, 1964.
13. **Bartels H, Moll W, Metcalfe J.** Physiology of gas exchange in the human placenta. *Am J Obstet Gynecol* 84: 1714–1730, 1962.
14. **Battaglia FC, Meschia G.** *An Introduction to Fetal Physiology*. London: Academic, 1986.
15. **Benirschke K, Kaufmann P, Baergen RN.** *Pathology of the Human Placenta* (5th ed.). New York: Springer, 2006.
16. **Berger R, Garnier Y.** Pathophysiology of perinatal brain damage. *Brain Res Rev* 30: 107–134, 1999.
17. **Bonel HM, Stolz B, Diedrichsen L, Frei K, Saar B, Tutschek B, Raio L, Surbek D, Srivastav S, Nelle M, Slotboom J, Wiest R.** Diffusion-weighted MR imaging of the placenta in fetuses with placental insufficiency. *Radiology* 257: 810–819, 2010.
18. **Borell U, Fernstrom I, Westman A.** Eine arteriographische studie des plazentarkreislaufs [Arteriographic study of placental circulation]. *Geburtshilfe Frauenheilkd* 18: 1–9, 1958.
19. **Burchell RC.** Arterial blood flow into the human intervillous space. *Am J Obstet Gynecol* 98: 303–11, 1967.
20. **Burton GJ.** The fine structure of the human placental villus as revealed by scanning electron microscopy. *Scanning Microsc* 1: 1811–1828, 1987.
21. **Burton GJ, Palmer ME.** Eradicating fetomaternal uid shift during perfusion fixation of the human placenta. *Placenta* 9: 327–332, 1988.
22. **Burton GJ, Ingram S, Palmer M.** The influence of mode of fixation on morphometrical data derived from terminal villi in the human placenta at term: a comparison of immersion and perfusion fixation. *Placenta* 8: 37–51, 1987.
23. **Burton GJ, Woods AW, Jauniaux E, Kingdom JC.** Rheological and physiological consequences of conversion of the maternal spiral arteries for uteroplacental blood flow during human pregnancy. *Placenta* 30: 473–482, 2009.
24. **Butler LA, Longo LD, Power GG.** Placental blood flows and oxygen transfer during uterine contractions: a mathematical model. *J Theor Biol* 61: 81–95, 1976.
25. **Chernyavsky IL.** *A Multiscale Analysis of Flow and Transport in the Human Placenta* (PhD. thesis). Nottingham, UK: Univ. Nottingham, 2011.
26. **Chernyavsky IL, Jensen OE, Leach L.** A mathematical model of intervillous blood flow in the human placentone. *Placenta* 31: 44–52, 2010.
27. **Chernyavsky IL, Leach L, Dryden IL, Jensen OE.** Transport in the placenta: homogenizing haemodynamics in a disordered medium. *Philos Trans A Math Phys Eng Sci* 369: 4162–4182, 2011.
28. **Costa A, Costantino ML, Fumero R.** Oxygen exchange mechanisms in the human placenta: mathematical modelling and simulation. *J Biomed Eng* 14: 385–389, 1992.
29. **Demené C, Pernot M, Biran V, Alison M, Fink M, Baud O, Tanter M.** Ultrafast Doppler reveals the mapping of cerebral vascular resistivity in neonates. *J Cereb Blood Flow Metab* 34: 1009–1017, 2014.
30. **Dymling SO, Persson HW, Hertz CH.** Measurement of blood perfusion in tissue using doppler ultrasound. *Ultrasound Med Biol* 17: 433–444, 1991.
31. **Egbor M, Ansari T, Morris N, Green CJ, Sibbons PD.** Pre-eclampsia and fetal growth restriction: how morphometrically different is the placenta? *Placenta* 27: 727–734, 2006
32. **Erian FF, Corrsin S, Davis SH.** Maternal, placental blood flow: a model with velocity-dependent permeability. *J Biomech* 10: 807–814, 1977.
33. **Eriksson JG, Kajantie E, Osmond C, Thornburg K, Barker DJ.** Boys live dangerously in the womb. *Am J Hum Biol* 22: 330–335, 2010.
34. **Faber JJ.** Application of the theory of heat exchangers to the transfer of inert materials in placentas. *Circ Res* 24: 221–34, 1969.
35. **Faber JJ.** Steady-state methods for the study of placental exchange. *Fed Proc* 36: 2640–2646, 1977.
36. **Faber JJ.** Review of flow limited transfer in the placenta. *Int J Obstet Anesth* 4: 230–237, 1995.
37. **Faber JJ, Anderson DF.** Model study of placental water transfer and causes of fetal water disease in sheep. *Am J Physiol Regul Integr Comp Physiol* 258: R1257–R1270, 1990.
38. **Faber JJ, Hart FM.** The rabbit placenta as an organ of diffusional exchange. Comparison with other species by dimensional analysis. *Circ Res* 19: 816–833, 1966.
39. **Faber JJ, Thornburg KL, Binder ND.** Physiology of placental transfer in mammals. *Integr Comp Biol* 32: 343–354, 1992.
40. **Felici M, Filoche M, Straus C, Similowski T, Sapoval B.** Diffusional screening in real 3D human acini a theoretical study. *Respir Physiol Neurobiol* 145: 279–293, 2005.
41. **Franke VE, Parker KH, Wee LY, Fisk NM, Sherwin SJ.** Time domain computational modelling of 1D arterial networks in monochorionic placentas. *ESAIM Math Model Numer Anal* 37: 557–580, 2003.
42. **Franken H.** Beitrag zur veranschaulichung von struktur und funktion der plazenta. *Zentralbl Gynakol* 76: 729–745, 1954.
43. **Freese UE.** The uteroplacental vascular relationship in the human. *Am J Obstet Gynecol* 101: 8–11, 1968.
44. **Freese UE.** Vascular relations of placental exchange areas in primates and man. In: *Respiratory Gas Exchange and Blood Flow in the Placenta*, edited by Longo LD, Bartels H. Bethesda, MD: Nat. Inst. Child Health Hum. Dev. . . . . ., 1972, p. 31–63.
45. **Freese UE, Ranniger K, Kaplan H.** The fetal-maternal circulation of the placenta. II. An X-ray cinematographic study of pregnant rhesus monkeys. *Am J Obstet Gynecol* 94: 361–366, 1966.
46. **Gill JS, Salafia CM, Grebenkov DS, Vvedensky DD.** Modeling oxygen transport in human placental terminal villi. *J Theor Biol* 291: 33–41, 2011.
47. **Ginsberg, MD, Myers RE.** Fetal brain damage following maternal carbon monoxide intoxication: an experimental study. *Acta Obstet Gynecol Scand* 53: 309–317, 1974.
48. **Gordon Z, Eytan O, Jaffa AJ, Elad D.** Fetal blood flow in branching models of the chorionic arterial vasculature. *Ann NY Acad Sci* 1101: 250–265, 2007.
49. **Gray H.** *Anatomy of the Human Body* (20th ed.). Philadelphia, PA: Lea & Febiger, 1918.
50. **Groome LJ.** A theoretical analysis of the effect of placental metabolism on fetal oxygenation under conditions of limited oxygen availability. *Biosystems* 26: 45–56, 1991.
51. **Guilbeau EJ, Renea DD.** Mathematical analysis of combined placental-fetal oxygen transport. *Adv Exp Med Biol* 37: 1007–1016, 1973.
52. **Guilbeau EJ, Reneau DD, Knisely MH.** The effects of placental oxygen consumption and the contractions of labor on fetal oxygen supply. A steady and unsteady state mathematical simulation. In: *Respiratory Gas Exchange and Blood Flow in the Placenta*, edited by Longo LD, Bartels H. Bethesda, MD: Nat. Inst. Child Health Hum. Dev., 1972, p. 297–344.
53. **Guilbeau EJ, Reneau DD, Knisely MH.** A detailed quantitative analysis of O_2 transport in the human placenta during steady and unsteady-state conditions. In: *Chemical Engineering Medicine. Advances in Chemistry*, edited by Reneau DD. Washington, DC: Am. Chem. Soc., vol. 118, chapt. 7, 1973, p. 130–171.
54. **Hafez SA, Borowicz P, Reynolds LP, Redmer DA.** Maternal and fetal microvasculature in sheep placenta at several stages of gestation. *J Anat* 216: 292–300, 2010.
55. **Heilmann L, Grebner H, Mattheck C, Ludwig H.** Mathematical, clinical, and laboratory study of hemodynamic changes in the placental circulation. *Arch Gynecol* 227: 303–313, 1979.
56. **Hellegers AE, Heller CJ, Behrman RE, Battaglia FC.** Oxygen and carbon dioxide transfer across the rhesus monkey placenta (macaca mulatta). *Am J Obstet Gynecol* 88: 22–31, 1964.
57. **Hill EP, Power GG, Longo LD.** A mathematical model of placental O_2 transfer with consideration of hemoglobin reaction rates. *Am J Physiol* 222: 721–729, 1972.
58. **Hill EP, Power GG, Longo LD.** A mathematical model of carbon dioxide transfer in the placenta and its interaction with oxygen. *Am J Physiol* 224: 283–299, 1973.
59. **Huen I, Morris DM, Wright C, Parker GJ, Sibley CP, Johnstone ED, Naish JH.** R 1 and R 2* changes in the human placenta in response to maternal oxygen challenge. *Magn Reson Med* 70: 1427–1433, 2013.

60. **Hutcheon JA, McNamara H, Platt RW, Benjamin A, Kramer MS.** Placental weight for gestational age and adverse perinatal outcomes. *Obstet Gynecol* 119: 1251–1258, 2012.
61. **Illsley NP, Fox H, Van der Veen F, Chawner L, Penfold P.** Human placental ultrastructure after in vitro dual perfusion. *Placenta* 6: 23–32, 1985.
62. **Jauniaux E, Jurkovic D, Campbell S.** Current topic: in vivo investigation of the placental circulations by Doppler echography. *Placenta* 16: 323–31, 1995.
63. **Jirkovská M, Smídová J, Frýda T.** Morphometric analysis of the vascularization of the terminal villi in normal and diabetic placenta. *Acta Stereol* 13: 43–47, 1994.
64. **Jirkovská M, Kubínová L, Janácek J, Moravcová M, Krejcí, V, Karen P.** Topological properties and spatial organization of villous capillaries in normal and diabetic placentas. *J Vasc Res* 39: 268–278, 2002.
65. **Jones NW, Hutchinson ES, Brownbill P, Crocker IP, Eccles D, Bugg GJ, Raine-Fenning NJ.** In vitro dual perfusion of human placental lobules as a flow phantom to investigate the relationship between feto-placental flow and quantitative 3D power doppler angiography. *Placenta* 30: 130–135, 2009.
66. **Kaplan AD, Jaffa AJ, Timor IE, Elad D.** Hemodynamic analysis of arterial blood flow in the coiled umbilical cord. *Reprod Sci* 17: 258–268, 2010.
67. **Kaufmann P.** Influence of ischemia and artificial perfusion on placental ultrastructure and morphometry. *Contrib Gynecol Obstet* 13: 18–26, 1985.
68. **Kaufmann P, Sen DK, Schweikhart G.** Classification of human placental villi. I. Histology. *Cell Tissue Res* 200: 409–423, 1979.
69. **King BF.** Comparative studies of structure and function in mammalian placentas with special reference to maternal-fetal transfer of iron. *Integr Comp Biol* 32: 331–342, 1992.
70. **Kirschbaum TH, Shapiro NZ.** A mathematical model of placental oxygen transfer. *J Theor Biol* 25: 380–402, 1969.
71. **Konje JC, Huppertz B, Bell SC, Taylor DJ, Kaufmann P.** 3-Dimensional colour power angiography for staging human placental development. *Lancet* 362: 1199–1201, 2003.
72. **Korteweg FJ, Erwich JJ, Holm JP, Ravisé JM, van der Meer J, Veeger NJ, Timmer A.** Diverse placental pathologies as the main causes of fetal death. *Obstet Gynecol* 114: 809–817, 2009.
73. **Laga EM, Driscoll SG, Munro HN.** Quantitative studies of human placenta. I. Morphometry. *Biol Neonate* 23: 231–259, 1973.
74. **Laga EM, Driscoll SG, Munro HN.** Human placental structure: relationship to fetal nutrition. In: *Problems Human Reproduction. Lactogen Hormones Fetal Nutrition Lactation*, edited by Josimovich JB, Reynolds M, Cobo E. London: John Wiley, 1974, vol. 2, p. 143–181.
75. **Lamport H.** The transport of oxygen in the sheep's placenta: the diffusion constant of the placenta. *Yale J Biol Med* 27: 26–34, 1954.
76. **Langheinrich AC, Wienhard J, Vormann S, Hau B, Bohle RM, Zygmunt M.** Analysis of the fetal placental vascular tree by X-ray micro-computed tomography. *Placenta* 25: 95–100, 2004.
77. **Langheinrich AC, Vorman S, Seidenstücker J, Kampschulte M, Bohle RM, Wienhard J, Zygmunt M.** Quantitative 3D micro-CT imaging of the human feto-placental vasculature in intrauterine growth restriction. *Placenta* 29: 937–941, 2008.
78. **Lardner TJ.** A model for placental oxygen exchange. *J Biomech* 8: 131–4, 1975.
79. **Lee R, Mayhew TM.** Star volumes of villi and intervillous pores in placentae from low and high altitude pregnancies. *J Anat* 186: 349–355, 1995.
80. **Leiser R, Kohler T.** The blood vessels of the cat girdle placenta. Observations on corrosion casts scanning electron microscopical and histological studies. I. Maternal vasculature. *Anat Embryol (Berl)* 167: 85–93, 1983.
81. **Leiser R, Kohler T.** The blood vessels of the cat girdle placenta. Observations on corrosion casts scanning electron microscopical and histological studies. II. Fetal vasculature. *Anat Embryol (Berl)* 170: 209–216, 1984.
82. **Leiser R, Krebs C, Ebert B, Dantzer V.** Placental vascular corrosion cast studies: a comparison between ruminants and humans. *Microsc Res Tech* 38: 76–87, 1997.
83. **Lewis RM, Brooks S, Crocker IP, Glazier J, Hanson MA, Johnstone ED, Panitchob N, Please CP, Sibley CP, Widdows KL, Sengers BG.** Review: modelling placental amino acid transfer from transporters to placental function. *Placenta* 34, *Suppl*: S46–51, 2013
84. **Linduska N, Dekan S, Messerschmidt A, Kasprian G, Brugger PC, Chalubinski K, Weber M, Prayer D.** Placental pathologies in fetal MRI with pathohistological correlation. *Placenta* 30: 555- 559, 2009.
85. **Longo LD.** Respiratory gas exchange. In: *Handbook of Physiolgoy. Respiratory System. Gas Exchange*, edited by Fishman AP, Farhi LE, Tenney SM, Geiger SR. Bethesda, MD: Am. Physol. Soc., sect. 3, vol. IV, 1987, p. 351- 401.
86. **Longo LD, Power GG.** Analyses of P_{O_2} and P_{CO_2} differences between maternal and fetal blood in the placenta. *J Appl Physiol* 26: 48–55, 1969.
87. **Longo LD, Power GG, Forster RE 2nd.** Placental diffusing capacity for carbon monoxide at varying partial pressures of oxygen. *J Appl Physiol* 26: 360–370, 1969.
88. **Longo LD, Hill EP, Power GG.** Theoretical analysis of factors affecting placental O_2 transfer. *Am J Physiol* 222: 730–739, 1972.
89. **Longo LD, Hill EP, Power GG.** Factors affecting placental oxygen transfer. In: *Respiratory Gas Exchange and Blood Flow in the Placenta*, edited by Longo LD, Bartels H. Bethesda, MD: Nat. Inst. Child Health Hum. Dev., 1972, p. 345–393.
90. **Longo LD, Hill EP, Power GG.** Factors affecting placental oxygen transfer. In: *Chemical Engineering Medicine*, edited by Reneau DD. Washington, DC: Am. Chem. Soc., 1973, chapt. 6, p. 88–129.
91. **Luckhardt M, Leiser R, Kingdom J, Malek A, Sager R, Kaisig C, Schneider H.** Effect of physiologic perfusion-fixation on the morphometrically evaluated dimensions of the term placental cotyledon. *J Soc Gynecol Investig* 3: 166–171, 1996.
92. **Mac Gabhann F, Popel AS.** Model of competitive binding of vascular endothelial growth factor and placental growth factor to VEGF receptors on endothelial cells. *Am J Physiol Heart Circ Physiol* 286: H153–H1564, 2004.
93. **Manganaro L, Fierro F, Tomei A, La Barbera L, Savelli S, Sollazzo P, Sergi ME, Vinci V, Ballesio L, Marini M.** MRI and DWI: feasibility of DWI and ADC maps in the evaluation of placental changes during gestation. *Prenat Diagn* 30: 1178–1184, 2010.
94. **Masselli G, Gualdi G.** MR imaging of the placenta: what a radiologist should know. *Abdom Imaging* 38: 573–587, 2013.
95. **Mauroy B, Filoche M, Weibel ER, Sapoval B.** An optimal bronchial tree may be dangerous. *Nature* 427: 633–636, 2004.
96. **Mayhew TM, Burton GJ.** Methodological problems in placental morphometry: apologia for the use of stereology based on sound sampling practice. *Placenta* 9: 565–581, 1988.
97. **Mayhew TM, Burton GJ.** Stereology and its impact on our understanding of human placental functional morphology. *Microsc Res Tech* 38: 195–205, 1997.
98. **Mayhew TM, Joy CF, Haas JD.** Structure-function correlation in the human placenta: the morphometric diffusing capacity for oxygen at full term. *J Anat* 139: 691–708, 1984.
99. **Mayhew TM, Jackson MR, Haas JD.** Microscopical morphology of the human placenta and its effects on oxygen diffusion: a morphometric model. *Placenta* 7: 121–131, 1986.
100. **Mayhew TM, Jackson MR, Haas JD.** Oxygen diffusive conductances of human placentae from term pregnancies at low and high altitudes. *Placenta* 11: 493- 503, 1990.
101. **Mayhew TM, Sørensen FB, Klebe JG, Jackson MR.** Oxygen diffusive conductance in placentae from control and diabetic women. *Diabetologia* 36: 955–960, 1993.
102. **Mayhew TM, Sørensen FB, Klebe JG, Jackson MR.** The effects of mode of delivery and sex of newborn on placental morphology in control and diabetic pregnancies. *J Anat* 183: 545–552, 1993
103. **Mayhew TM, Wijesekara J, Baker PN, Ong SS.** Morphometric evidence that villous development and fetoplacental angiogenesis are compromised by intrauterine growth restriction but not by pre-eclampsia. *Placenta* 25: 829–833, 2004.
104. **Meschia G, Battaglia FC, Bruns PD.** Theoretical and experimental study of transplacental diffusion. *J Appl Physiol* 22: 1171–1178, 1967.
105. **Meschia G, Cotter JR, Makowski EL, Barron DH.** Simultaneous measurement of uterine and umbilical blood flows and oxygen uptakes. *Q J Exp Physiol Cogn Med Sci* 52: 1–18, 1967.
106. **Metcalfe J, Romney SL, Ramsey LH, Reid DE, Burwell CS.** Estimation of uterine blood flow in normal human pregnancy at term. *J Clin Invest* 34: 1632–1638, 1955.
107. **Metcalfe J, Moll W, Bartels H.** Gas exchange across the placenta. *Fed Proc* 23: 774–780, 1964.

108. **Middleman, S.** *Transport Phenomena in the Cardiovascular System*. New York: Wiley-Interscience, 1972.
109. **Misra DP, Salafia CM, Charles AK, Miller RK.** Placental measurements associated with intelligence quotient at age 7 years. *J Dev Orig Health Dis* 3: 190–197, 2012.
110. **Moll W.** Gas exchange in concurrent, countercurrent and crosscurrent flow systems. In: *Respiratory Gas Exchange and Blood Flow in the Placenta*, edited by Longo LD, Bartels H. Bethesda, MD: Nat. Inst. Child Health Hum. Dev., 1972, p. 281-96.
111. **Moore RJ, Issa B, Tokarczuk P, Duncan KR, Boulby P, Baker PN, Bowtell RW, Worthington BS, Johnson IR, Gowland PA.** In vivo intravoxel incoherent motion measurements in the human placenta using echo-planar imaging at 0.5 T. *Magn Reson Med* 43: 295–302, 2000.
112. **Moore RJ, Strachan BK, Tyler DJ, Duncan KR, Baker PN, Worthington BS, Johnson IR, Gowland PA.** In utero perfusing fraction maps in normal and growth restricted pregnancy measured using IVIM echo-planar MRI. *Placenta* 21: 726–732, 2000.
113. **Morel O, Pachy F, Chavatte-Palmer P, Bonneau M, Gayat E, Laigre P, Evain-Brion D, Tsatsaris V.** Correlation between uteroplacental three-dimensional power Doppler indices and true uterine blood flow: evaluation in a pregnant sheep model. *Ultrasound Obstet Gynecol* 36: 635–40, 2010.
114. **Morel O, Grangé G, Fresson J, Schaaps JP, Foidart JM, Cabrol D, Tsatsaris V.** Vascularization of the placenta and the sub-placental myometrium: feasibility and reproducibility of a three-dimensional power Doppler ultrasound quantification technique. A pilot study. *J Matern Fetal Neonatal Med* 24: 284–290, 2011.
115. **Mossman HW.** The rabbit placenta and the problem of placental transmission. *Am J Anat* 37: 433–497, 1926.
116. **Nguyen D, Nguyen C, Yacobozzi M, Bsat F, Rakita D.** Imaging of the placenta with pathologic correlation. *Semin Ultrasound CT MR* 33: 65-77, 2012.
117. **Panigel M, Pascaud M.** Les orifices artéeriels d'entrée du sang maternel dans la chambre intervilleuse du placenta humain. *Bull Assoc Anat 53rd Congr* 142: 1968, p. 1287–1298.
118. **Panitchob N, Widdows KL, Crocker IP, Hanson MA, Johnstone ED, Please CP, Sibley CP, Glazier JD, Lewis RM, Sengers BG.** Computational modelling of amino acid exchange and facilitated transport in placental membrane vesicles. *J Theor Biol* 365C: 352–364, 2014.
119. **Perry RH, Green DW.** *Perry's Chemical Engineers Handbook* (7th ed.). New York: McGraw-Hill, 1997.
120. **Power GG, Jenkins F.** Factors affecting O_2 transfer in sheep and rabbit placenta perfused in situ. *Am J Physiol* 229: 1147–1153, 1975.
121. **Power GG, Longo LD.** Graphical analysis of maternal and fetal exchange of O_2 and CO_2. *J Appl Physiol* 26: 38–47, 1969.
122. **Power GG, Longo LD.** Fetal circulation times and their implications for tissue oxygenation. *Gynecol Invest* 6: 342–355, 1975.
123. **Power GG, Hill EP, Longo LD.** Analysis of uneven distribution of diffusing capacity and blood flow in the placenta. *Am J Physiol* 222: 740–746, 1972.
124. **Power GG, Hill EP, Longo LD.** A mathematical model of carbon dioxide transfer in the placenta. In: *Respiratory Gas Exchange and Blood Flow in the Placenta*, edited by Longo LD, Bartels H. Bethesda, MD: Nat. Inst. Child Health Hum. Dev., 1972, p. 395–418.
125. **Ragavendra N, Tarantal AF.** Intervillous blood flow in the third trimester gravid rhesus monkey (Macaca mulatta): use of sonographic contrast agent and harmonic imaging. *Placenta* 22: 200–205, 2001.
126. **Ramsey EM.** Circulation in the intervillous space of the primate placenta. *Am J Obstet Gynecol* 84: 164916–63, 1962.
127. **Ramsey EM, Corner GW, Donner MW.** Serial and cineradioangiographic visualization of maternal circulation in the primate (hemochorial) placenta. *Am J Obstet Gynecol* 86: 213–225, 1963.
128. **Ranck JB, Windle WF.** Brain damage in the monkey, macaca mulatta, by asphyxia neonatorum. *Exp Neurol* 1: 130–154, 1959.
129. **Rankin JH.** The effects of shunted and unevenly distributed blood flows on crosscurrent exchange in the sheep placenta. In: *Respiratory Gas Exchange and Blood Flow in the Placenta*, edited by Longo LD, Bartels H. Bethesda, MD: Nat. Inst. Child Health Hum. Dev., 1972, p. 207–229.
130. **Rankin JH, Peterson EN.** Application of the theory of heat exchangers to a physiological study of the goat placenta. *Circ Res* 24: 235–250, 1969.
131. **Rasmussen AS, Lauridsen H, Laustsen C, Jensen BG, Pedersen SF, Uhrenholt L, Boel LW, Uldbjerg N, Wang T, Pedersen M.** High-resolution ex vivo magnetic resonance angiography: a feasibility study on biological and medical tissues. *BMC Physiol* 10: 3, 2010.
132. **Rees S, Inder T.** Fetal and neonatal origins of altered brain development. *Early Hum Dev* 81: 753–761, 2005.
133. **Rejniak KA, Kliman HJ, Fauci LJ.** A computational model of the mechanics of growth of the villous trophoblast bilayer. *Bull Math Biol* 66: 199–232, 2004.
134. **Reneau DD, Guilbeau EJ, Cameron JM.** A theoretical analysis of the dynamics of oxygen transport and exchange in the placentalfetal system. *Microvasc Res* 8: 346–361, 1974.
135. **Rennie MY, Whiteley KJ, Kulandavelu S, Adamson SL, Sled JG.** 3D visualisation and quantification by microcomputed tomography of late gestational changes in the arterial and venous fetoplacental vasculature of the mouse. *Placenta* 28: 833- 840, 2007.
136. **Rennie MY, Detmar J, Whiteley KJ, Jurisicova A, Adamson SL, Sled JG.** Expansion of the fetoplacental vasculature in late gestation is strain dependent in mice. *Am J Physiol Heart Circ Physiol* 302: H1261–H1273, 2012.
137. **Resta L, Capobianco C, Marzullo A, Piscitelli D, Sanguedolce F, Schena FP, Gesualdo L.** Confocal laser scanning microscope study of terminal villi vessels in normal term and preeclamptic placentas. *Placenta* 27: 735–739, 2006.
138. **Roughton FJ, Forster RE.** Relative importance of diffusion and chemical reaction rates in determining rate of exchange of gases in the human lung, with special reference to true diffusing capacity of pulmonary membrane and volume of blood in the lung capillaries. *J Appl Physiol* 11: 290–302, 1957.
139. **Rubin JM, Adler RS, Fowlkes JB, Spratt S, Pallister JE, Chen JF, Carson PL.** Fractional moving blood volume: estimation with power Doppler US. *Radiology* 197: 183–190, 1995.
140. **Salafia CM, Zhang J, Charles AK, Bresnahan M, Shrout P, Sun W, Maas EM.** Placental characteristics and birthweight. *Paediatr Perinat Epidemiol* 22: 229–239, 2008.
141. **Salomon LJ, Siauve N, Balvay D, Cuénod CA, Vayssettes C, Luciani A, Frija G, Ville Y, Clément O.** Placental perfusion MR imaging with contrast agents in a mouse model. *Radiology* 235: 73- 80, 2005.
142. **Sapoval B, Filoche M, Weibel ER.** Smaller is better–but not too small: a physical scale for the design of the mammalian pulmonary acinus. *Proc Natl Acad Sci USA* 99: 10411–10416, 2002.
143. **Schmid-Schönbein H.** Conceptional proposition for a specific microcirculatory problem: maternal blood flow in hemochorial multivillous placentae as percolation of a "porous medium". *Trophobl Res* 3: 17–38, 1988.
144. **Schneider H.** Tolerance of human placental tissue to severe hypoxia and its relevance for dual ex vivo perfusion. *Placenta* 30, *Suppl* A: S71-6, 2009.
145. **Schröder H.** Structural and functional organization of the placenta from the physiological point of view. In: *Structure Function Organ Placenta*, edited by Kaufmann P, King BF. Karger, Basel, Switzerland: Karger, 1982, p. 4–12.
146. **Sen DK, Kaufmann P, Schweikhart G.** Classification of human placental villi. II. Morphometry. *Cell Tissue Res* 200: 425–434, 1979
147. **Sengers BG, Please CP, Lewis RM.** Computational modelling of amino acid transfer interactions in the placenta. *Exp Physiol* 95: 829–840, 2010.
148. **Sengupta A, Biswas P, Jayaraman G, Guha SK.** Understanding utero-placental blood flow in normal and hypertensive pregnancy through a mathematical model. *Med Biol Eng Comput* 35: 223–230, 1997.
149. **Serov AS.** *Modeling Oxygen Transport in the Human Placenta* (PhD thesis). Palaiseau, France: Laboratoire de Physique de la Matiére Condensée École Polytechnique, 2015 [https://tel.archives-ouvertes.fr/tel-01205237/].
150. **Serov AS, Salafia CM, Brownbill P, Grebenkov DS, Filoche M.** Optimal villi density for maximal oxygen uptake in the human placenta. *J Theor Biol* 364: 383–396, 2015.
151. **Serov AS, Salafia CM, Filoche M, Grebenkov DS.** Analytical theory of oxygen transfer in the human placenta. *J Theor Biol* 368: 133–144, 2015.
152. **Shapiro NZ, Kirschbaum TH, Assali NS.** Mental exercises in placental transfer. *Am J Obstet Gynecol* 97: 130–137, 1967.
153. **Sørensen A, Peters D, Fründ E, Lingman G, Christiansen O, Uldbjerg N.** Changes in human placental oxygenation during maternal hyperoxia estimated by blood oxygen level-dependent magnetic resonance imaging (BOLD MRI). *Radiology* 42: 310–314, 2013.
154. **Sørensen A, Peters D, Simonsen C, Pedersen M, Stausbøl-Grøn B, Christiansen OB, Lingman G, Uldbjerg N.** Changes in human fetal

oxygenation during maternal hyperoxia as estimated by BOLD MRI. *Prenat Diagn* 33: 141–145, 2013.

155. **Stevenson GN, Collins SL, Welsh AW, Impey LW, Noble JA.** A technique for the estimation of fractional moving blood volume by using three-dimensional power doppler US. *Radiology* 274: 132363, 2015.
156. **Talbert DG, Sebire NJ.** The dynamic placenta: I. Hypothetical model of a placental mechanism matching local fetal blood flow to local intervillus oxygen delivery. *Med Hypotheses* 62: 511–519, 2004.
157. **Teasdale F.** Morphometric evaluation. In: *Contributions to Gynecology Obstetrics. Morphology Function Aspiration Placental Dysfunction*, edited by Soma H. Basel, Switzerland: Karger, 1982, vol. 9, p. 17–28.
158. **Teasdale F.** Histomorphometry of the human placenta in Class B diabetes mellitus. *Placenta* 4: 1–12, 1983.
159. **Teng J, Chang T, Reyes C, Nelson KB.** Placental weight and neurologic outcome in the infant: a review. *J Matern Fetal Neonatal Med* 25: 2082–2087, 2012.
160. **Thoumsin HJ, Albert A, Duvivier J.** Preliminary clinical application of a mathematical model for interpreting dehydroepiandrosterone-sulfate loading test in late pregnancy. *J Perinat Med* 6: 32–38, 1978.
161. **van den Wijngaard JP, Westerhof BE, Ross MG, van Gemert MJ.** A mathematical model of twin-twin transfusion syndrome with pulsatile arterial circulations. *Am J Physiol Regul Integr Comp Physiol* 292: R1519–R1531, 2007.
162. **Weibel ER.** Morphometry and lung models. In: *Quantitative Methods Morphology/Quantitative Methoden der Morphology*, edited by Weibel ER, Elias H. Berlin, Germany: Springer, 1967, p. 253–267.
163. **Weibel ER.** Morphometric estimation of pulmonary diffusion capacity. I. Model and method. *Respir Physiol* 11: 54–75, 1970.
164. **Weibel ER, 1984.** *The Pathway for Oxygen*. Cambridge, MA: Harvard Univ. Press, 1984.
165. **Weibel ER.** What makes a good lung? *Swiss Med Wkly* 139: 375–386, 2009.
166. **West JB.** *Respiratory Physiology: The Essentials* (8th ed.). Baltimore, MD: Lippincott Williams & Wilkins, 2008.
167. **Wilbur WJ, Power GG, Longo LD.** Water exchange in the placenta: a mathematical model. *Am J Physiol Regul Integr Comp Physiol* 235: R181–R199, 1978.
168. **Wilkening RB, Meschia G.** Current topic: comparative physiology of placental oxygen transport. *Placenta* 13: 1–15, 1992.
169. **Wilkin P.** Les theories explicatives du mecanisme desechanges transplacentaires. In: *Le Placenta Human*, edited by Snoeck J. Paris: Masson et Cie Paris, 1958, p. 248–279.
170. **Yeh BM.** Has the time arrived to image placental perfusion? *Radiology* 241: 633–634, 2006.